Mol Neurobiol (2012) 46:205–216
DOI 10.1007/s12035-012-8308-3

A New Link to Mitochondrial Impairment in Tauopathies

Kathrin L. Schulz · Anne Eckert · Virginie Rhein · Sören Mai · Winfried Haase · Andreas S. Reichert · Marina Jendrach · Walter E. Müller · Kristina Leuner

Received: 15 May 2012 / Accepted: 12 July 2012 / Published online: 31 July 2012

Abstract Tauopathies like the "frontotemporal dementia with Parkinsonism linked to chromosome 17" (FTDP-17) are characterized by an aberrant accumulation of intracellular neurofibrillary tangles composed of hyperphosphorylated tau. For FTDP-17, a pathogenic tau mutation P301L was identified. Impaired mitochondrial function including disturbed dynamics such as fission and fusion are most likely major pathomechanisms of most neurodegenerative diseases. However, very little is known if tau itself affects mitochondrial function and dynamics. We addressed this question using SY5Y cells stably overexpressing wild-type (wt) and P301L mutant tau. P301L overexpression resulted in a substantial complex I deficit accompanied by decreased ATP levels and increased susceptibility to oxidative stress. This was paralleled by pronounced changes in mitochondrial morphology, decreased fusion and fission rates accompanied by reduced expression of several fission and fusion factors like OPA-1 or DRP-1. In contrast, overexpression of wt tau exhibits protective effects on mitochondrial function and dynamics including enhanced complex I activity. Our findings clearly link tau bidirectional to mitochondrial function and dynamics, identifying a novel aspect of the physiological role of tau and the pathomechanism of tauopathies.

Keywords Taupathy · Mitochondrial impairment · FTDP-17 · Mitochondrial morphology

K. L. Schulz · W. E. Müller · K. Leuner (✉)
Department of Pharmacology, ZAFES, Biocenter,
University of Frankfurt,
60438 Frankfurt, Germany
e-mail: leuner@pharmtech.uni-erlangen.de

A. Eckert · V. Rhein
Neurobiology Laboratory for Brain Aging and Mental Health,
Associated Research Group Department of Biomedicine,
Psychiatric University Clinics, University of Basel,
4025 Basel, Switzerland

S. Mai · M. Jendrach
Kinematic Cell Research Group,
Institute for Cell Biology and Neuroscience, Center of Excellence
Frankfurt, Macromolecular Complexes, University of Frankfurt,
60438 Frankfurt, Germany

W. Haase
Department of Structural Biology,
Max Planck Institute of Biophysics,
60438 Frankfurt, Germany

A. S. Reichert
Mitochondrial Biology, Buchmann Institute of Molecular
Life Science, Goethe University Frankfurt am Main,
Fachbereich Medizin,
Max-von-Laue-Strasse 15,
60438 Frankfurt, Germany

Introduction

The pathological hallmark of tauopathies is an aberrant intracellular accumulation of neurofibrillary tangles (NFTs) which are characteristic for several neurodegenerative disease including Alzheimer disease (AD) [1]. NFTs are built up by paired helical filaments (PHFs) composed of hyperphosphorylated tau protein, one of the microtubule-associated proteins (MAPs) [2], which plays a crucial role in microtubule dynamics. Tau stabilizes microtubules and the dynamic equilibrium between free and bound tau is regulated through phosphorylation and dephosphorylation. Recently, an important role of tau for retrograde and anterograde transport was discovered [3]. In the specific tauopathy FTDP-17 (frontotemporal dementia with Parkinsonism linked to chromosome 17) several mutations of the tau gene have been identified which are causative for

neurodegeneration and dementia [4–6]. Two of the pathogenic tau mutations found in FTDP-17, ΔK280 and P301L, have a much stronger tendency for PHF aggregation compared to wild type tau [7]. A previous study of our group with P301L transgenic mice revealed mitochondrial dysfunction mainly associated with a complex I defect leading to impaired mitochondrial respiration and reduced ATP synthesis in mouse brains during aging [8]. As impaired mitochondrial function and enhanced oxidative stress represent a common pathomechanism in a large number of neurodegenerative diseases [9, 10], identifying a potential direct impact of tau pathology for mitochondrial dysfunction may be of major relevance.

Mitochondria are dynamic organelles undergoing continuous cycles of fission and fusion, which is discussed as a rescue mechanism and important for maintaining the integrity of mitochondria through exchange of metabolites as well as proteins and for segregation and protection of mitochondrial DNA (mtDNA) [11–14]. Cell function and survival is negatively affected by a loss of the tightly controlled balance between fission and fusion, promoting either excessive fission or fusion. Increased fusion leads to mitochondrial elongation and excess of fission to fragmentation, both resulting in impaired mitochondrial function. These defects might result in decreased mitochondrial motility, decreased energy production, and enhanced oxidative stress. In mammalian cells, several dynamin-related GTPases regulate fission and fusion processes. For fusion, OPA1, MFN1 and MFN2 are required, whereas fission involves DRP1, FIS1 and MEF1 [15, 16]. Impairment of mitochondrial dynamics such as fission and fusion are currently considered to play an important role in neurodegenerative diseases [17]. Recently, abnormal fission and fusion were linked to elevated Aβ levels using AD fibroblasts [18] and a human neuroblastoma cell line as a model for AD [19]. However, it is still unclear whether and how tau pathology is linked to alterations of mitochondrial function and dynamics.

To address this important question we investigated the effects of the overexpression of wild type (wt) and P301L mutant tau (P301L) on mitochondrial dynamics and function in a previously described model system, namely a neuronal S5Y5 cell line stably overexpressing wt and P301L tau protein [20].

We show that the expression of the tau mutation P301L results in a considerable complex I deficit accompanied by decreased ATP levels, and an increased susceptibility to oxidative stress. These functional deficits were paralleled by pronounced changes in mitochondrial morphology and decreased fission and fusion suggesting a causative relationship. In contrast, overexpression of wt tau exhibits protective effects on mitochondrial function and morphology.

Results

P301L Neuroblastoma Cells Exhibit Mitochondrial Respiratory Deficits

In our cell model, stable transfection of SH-SY5Y cells with the expression vector pRc/RSV, which was either empty (control) or harbouring expression constructs encoding the longest 4-repeat isoform of human tau without (wt) or with the pathogenic FTDP-17 mutation P301L (P301L), did not modify morphology of the cells as previously described [21]. Human tau expression was substantially increased in wt as well as P301L overexpressing SH-SY5Y cells in comparison to control cells bearing the empty vector (Fig. 1a,b) and similar levels were expressed in wt and P301L cells confirming previous findings [20].

To address whether tau affects mitochondrial respiratory function we determined the activities of different respiratory chain complexes in isolated mitochondria from wt and P301L overexpressing SY5Y cells and compared those to control cells. For normalization of the activities of the respiratory chain complexes, we determined the citrate synthase (CS) activity to standardize assay results [22]. Consistent with previous experiments in transgenic mice [8] we found a substantially diminished complex I activity in P301L cells (Fig. 1c). In contrast, wt overexpressing cells showed an increased complex I activity. Regarding the other complex activities, wt tau and the P301L mutation showed increased

Fig. 1 Expression of tau protein and altered activities of the respiratory chain complexes in Wt tau and P301L cells. **a** Human tau expression levels of SH-SY5Y cells were detected by Western Blotting using phosphorylation-independent human tau antibody HT7 antibody (aa 159–163) indicating strong expression of 4R-tau (~60–65 kDa band) in wt and P301L transfected cells compared to control cells. Wt and P301L cells show similar 4R-tau expression levels. In addition, low molecular tau levels (~28 kDa) were increased in wt and P301L cells. **b** Human tau detected by immunochemistry using likewise HT7 antibody indicates a stronger presence of tau in wt and P301L cells compared to the endogenous expression in control cells. **c**–**f** The different complex activities were measured in isolated mitochondria and the activities are expressed in nmol/min/mg. All complex activities were normalized to the citrate synthase activity of the mitochondrial preparation and are given as Complex/CS ratio. **c** Complex I activity was determined using DBQ and NADH as substrates and NADH oxidation rates were recorded. **d** The activity of complex II was measured by following the decrease in absorbance at 600 nm resulting from the reduction of DCIP. **e** The oxidation of decylubiquinol obtained by complex III was determined using cytochrome *c* as an electron acceptor and the enzyme activity was measured at 550 nm. **f** The activity of complex IV was determined using a colorimetric assay, which is based on the observation that a decrease in absorbance at 550 nm of ferrocytochrome *c* is caused by its oxidation to ferricytochrome *c* by cytochrome *c* oxidase. **c**–**f** Data are mean±SEM, $n=3$–5; unpaired *t*-test, ***$p<0.001$

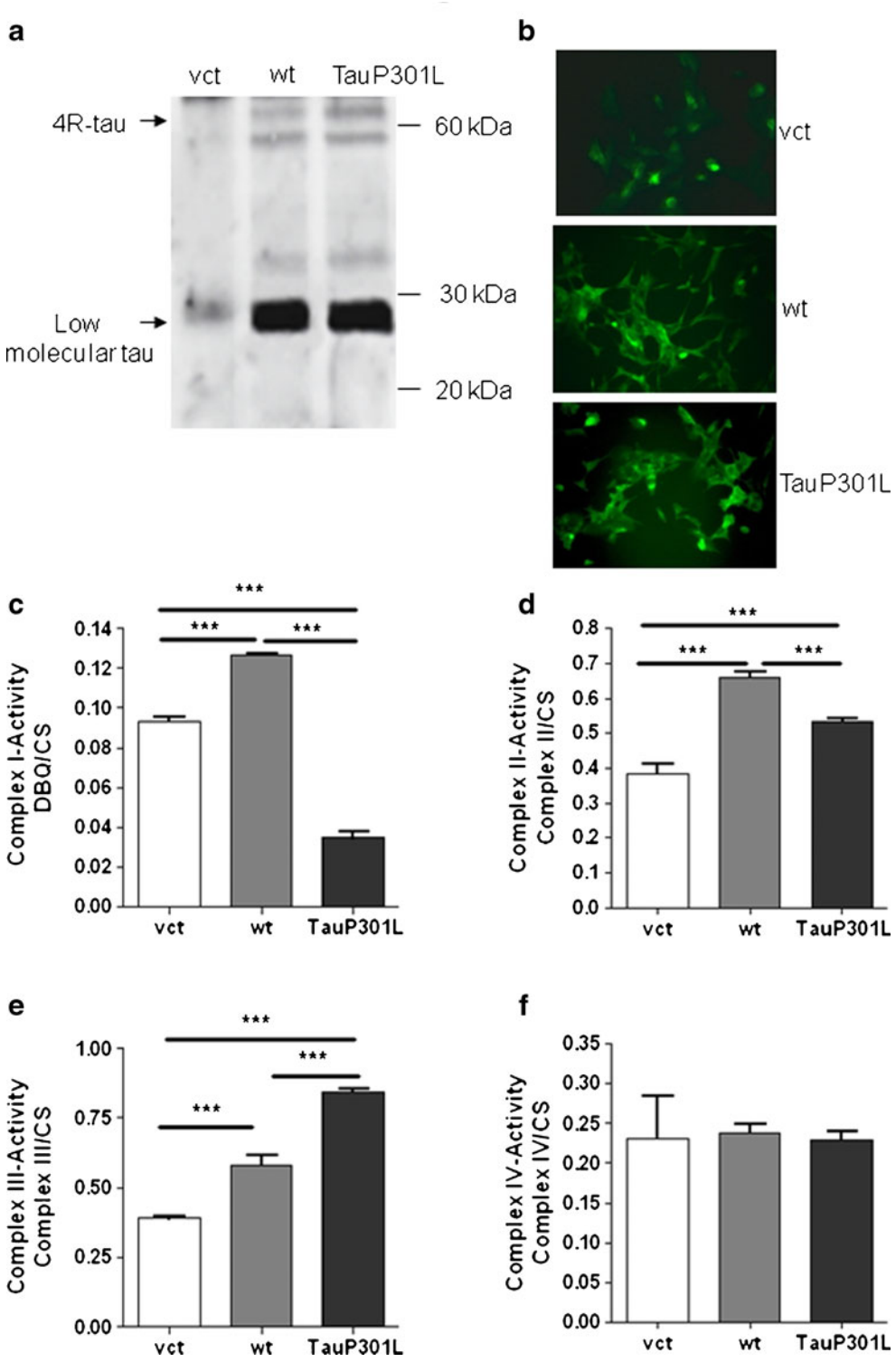

activity of succinate dehydrogenase (complex II, Fig. 1d) and of ubiquinol cytochrome *c* reductase (complex III, Fig. 1e) but to a different extent. In contrast, complex IV activity was not altered compared to vector control (Fig. 1f).

The P301L Tau Mutation Impairs Mitochondrial Function

As mitochondria strictly regulate several cellular functions from generating ATP to apoptosis, a loss of integrity and complex I activity is considered to play an important role in

aging and developing neurodegenerative diseases [23]. Accordingly, ATP levels, mitochondrial membrane potential (MMP), compensation of oxidative stress, and other mitochondrial parameters were also affected by the overexpression of wt and P301L tau in SH-SY5Y cells again in a bidirectional way. Wt tau expression significantly increased metabolic activity (Fig. 2a). ATP levels in these cells and MMP were also increased (Fig. 2b, c). In contrast, P301L expression decreased metabolic activity as well as ATP levels even compared to control cells and also diminishes MMP back to control level with a slightly additional reduction (Fig. 2a–c).

In order to determine if these alterations in mitochondrial functions were caused by a change in the mitochondrial mass, we investigated by real time PCR the mtDNA content according to Bai et al. [24], who positively correlated an increase in mtDNA content with mitochondrial proliferation. We did not detect any differences in mtDNA content between the three cell types and conclude therefore that mitochondrial mass is not altered after expression of wt and mutant tau (Fig. 2d).

Next, we asked whether the altered mitochondrial function in P301L cells leads to elevated sensitivity to oxidative stress. After incubation with H_2O_2 P301L cells showed significant lower metabolic activity (Fig. 3a), reduced ATP levels (Fig. 3b) and a depolarized membrane potential (Fig. 3c) compared to control and wt tau cells, indicating an increased sensitivity against oxidative stress. On the other hand, overexpression of wt tau seems to be protective against oxidative stress. These cells respond less to H_2O_2 induced loss of metabolic activity, decreased ATP levels and show only the same slightly depolarization than the control cells.

Ultrastructure of Mitochondria Reflects Their Functional Insufficiency

Alterations in the arrangement of the respiratory chain complexes are often coupled to changes in the mitochondrial ultrastructure and are dependent on the structural integrity of the inner mitochondrial membrane [25]. Lately, Baloyannis and colleagues revealed a change in mitochondrial morphology during Alzheimer's disease (reviewed by Baloyannis [26]). To investigate whether overexpression of wt tau or mutant P301L tau affects the ultrastructure of mitochondria

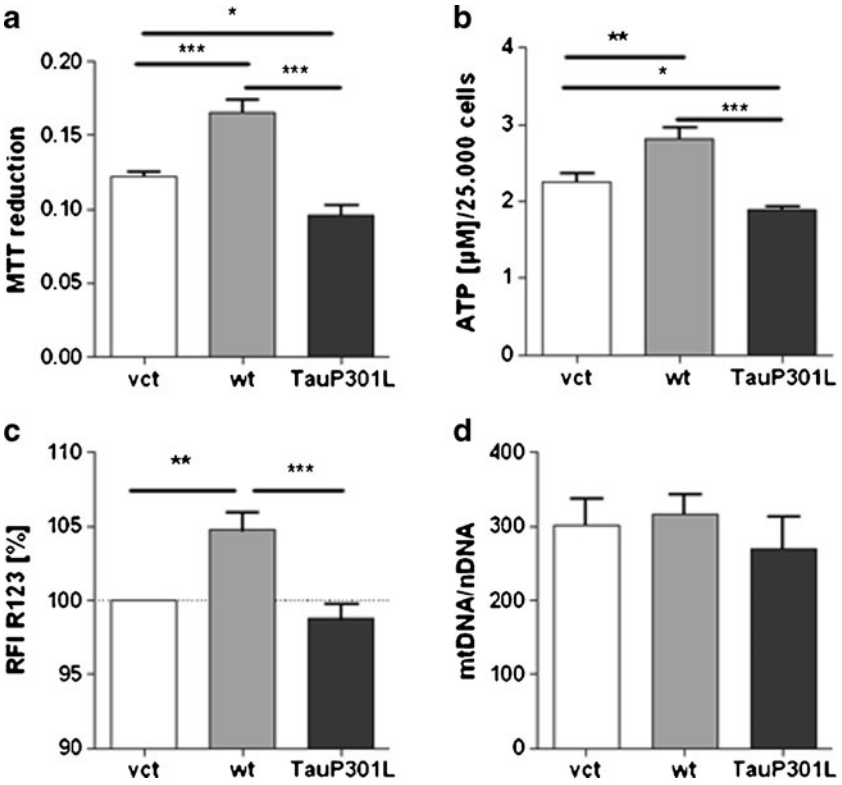

Fig. 2 Overexpression of Wt and mutant tau alters mitochondrial function. **a** Cells were seeded the day before at a density of 2.5×10^4 per well to measure the metabolic activity using the MTT test. Data are mean±SEM, $n=6$; unpaired t-test, $^*p<0.05$, $^{***}p<0.001$. **b** Basal ATP levels in SY5Y vct, wt tau and P301L tau cells were analyzed using a bioluminescence assay (ViaLight). Cells were seeded the day before at a density of 2.5×10^4 per well. Data are mean±SEM, $n=6$; unpaired t-test, $^*p<0.05$, $^{**}p<0.01$, $^{***}p<0.001$. **c** MMP was investigated by staining cells with the membrane potential-sensitive fluorescence dye R123. Cells were plated the day before at a density of 10×10^5 per well. Data are mean±SEM, $n=14$, unpaired t-test $^{**}p<0.01$, $^{***}p<0.001$. **d** Using real-time PCR, we determined the mtDNA copies compared to nDNA copies and revealed no differences between the SH-SY5Y cell lines. As the amount of mtDNA correlates positively with the number of mitochondria we conclude that there is no variation in the number of mitochondria in SH-SY5Y cells. Data are mean±SEM, $n=4$

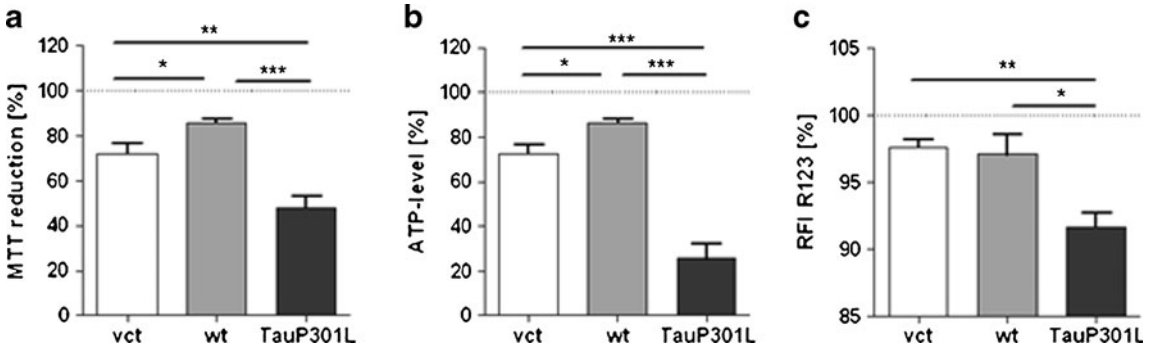

Fig. 3 P301L Cells are More Vulnerable against Oxidative Stress. SH-SY5Y cells were seeded the day before the experiment occurred and then incubated for additional 24 h with 100 μM H_2O_2 to measure different parameters reflecting mitochondrial function. **a** Metabolic activity was detected using the MTT test in SY5Y vct, wt tau and P301L cells. Data are mean±SEM, n=4–7, unpaired t-test *p<0.05, **p<0.01, ***p<0,001. **b** ATP levels in SY5Y vct, wt tau and P301L tau cells were measured after incubation with 100 μM H_2O_2 for 24 h. Data are mean±SEM, n=4–7, unpaired t-test *p<0.05, ***p<0,001. **c** The mitochondrial membrane potential was determined using the cationic dye rhodamine123 (*RFI* relative fluorescence intensity). After the preincubation with 100 μM H_2O_2 for 24 h, cells were incubated for 15 min with R123 and fluorescence was detected. Data are mean± SEM, n=4–7; unpaired t-test, *p<0.05, **p<0.01

in SH-SY5Y cells, we performed electron microscopy. The mitochondrial ultrastructure of cells stable transfected with vector control or with wt tau appeared normal showing typical cristae (Fig. 4a, b). In contrast, the cristae morphology of P301L mitochondria showed globular structures and branched cristae membranes (Fig. 4c). These alterations in cristae morphology upon overexpression of mutant P301L tau are consistent with the observed mitochondrial dysfunction characterized by reduced ATP levels and impaired oxidative phosphorylation.

Mutated Tau Impairs the Distribution and Dynamics of Mitochondria

The physiological role of tau is to stabilize the microtubule network, which is responsible for an appropriate morphology of neurons and the kinesin/dynein transport machinery. Bunker et al. [27] showed, that the P301L mutation exhibits markedly reduced abilities to regulate the dynamic instability of microtubules relative to tau. As a consequence from the destabilization of the microtubule network also the transport of vesicles and organelles, such as mitochondria, are disturbed [28, 29]. As the distribution of mitochondria can severely impact cellular metabolism, we used MitoTracker CMXRos to visualize the distribution and morphology of mitochondria in SH-SY5Y cells. Control cells showed long tubular mitochondria, which were partly interconnected, and some clustering of mitochondria around the nucleus (Fig. 5a). The overexpression of wt tau led to a widely connected network and showed only few mitochondrial clusters. In contrast, in P301L cells nearly all mitochondria were clustered around the nucleus. Furthermore, their cell body seemed to be constricted and globular, whereas the cell bodies of wt tau cells were thin and comprehensive. To confirm that the different distribution of mitochondria is connected to the tau mutations, the dynamics of mitochondria were analyzed in SH-SY5Y cells. Live cell imaging over 2 min was performed with MitoTracker Deep Red stained mitochondria and the time dependent change in maximum fluorescence intensity was compared to the first picture to determine mitochondrial movements. The P301L cells revealed significant less mitochondrial movements compared to control cells and wt cells (Fig. 5b), correlating with their perinuclear

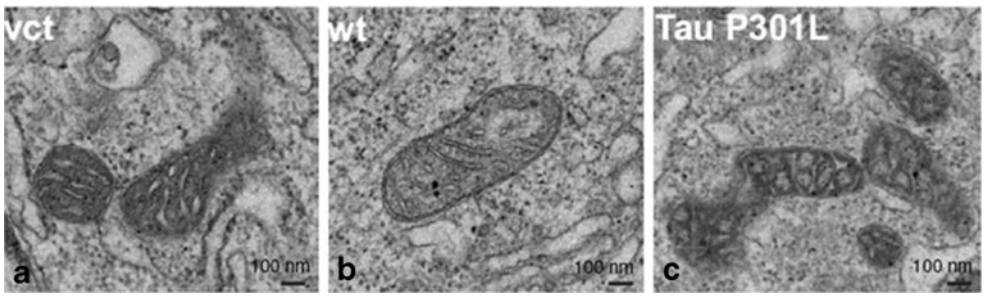

Fig. 4 The Overexpression of Wt tau and the P301L mutation causes changes in the mitochondrial ultrastructure. Ultrastructure of mitochondrial sections of SH-SY5Y cells stably expressing a vector control (**a**, vct), wt tau (**b**) or mutant P301L tau (**c**, P301L). Electron micrographs of sections of chemically fixed cells are shown. Scale bar=100 nm

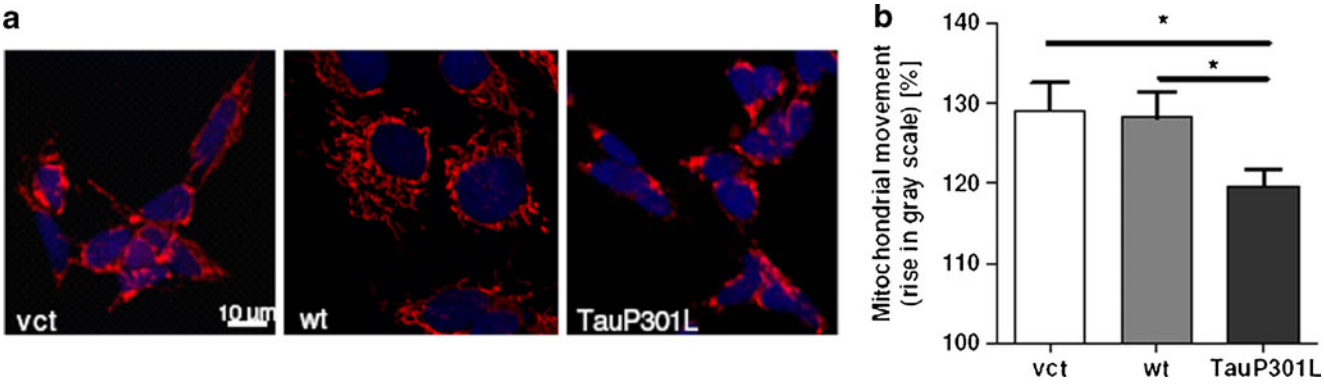

Fig. 5 Distribution and dynamics of mitochondria in P301L cells are disturbed. SH-SY5Y cells were loaded with MitoTracker Deep Red and live confocal imaging was conducted. **a** Example of confocal images that revealed changes in the mitochondrial morphology after fixation of SH-SY5Y cells with 4 % PFA and stained mitochondria with MitoTracker CMXRos (*red*) (*blue*, Hoechst-staining of the nucleus). **b** Live cell imaging of mitochondria stained with MitoTracker Deep Red were recorded over 2 min (one picture every 1.5 s) to study mitochondrial dynamics. Data are mean±SEM, $n=13–18$; unpaired *t*-test, $*p<0.05$

aggregation, whereas the wt tau cells showed no differences to control cells. In conclusion, P301L tau expression impairs mitochondrial transport and motility.

Aberrant Fission and Fusion in P301L Cells

Mitochondrial movement is the prerequisite for fission and fusion, which are discussed to play an important role for mitochondrial integrity, as proteins and mtDNA can be exchanged between damaged and healthy mitochondria to ensure cell survival [11, 13]. As reduced mitochondrial dynamics could contribute to the observed deficiencies of P301L cells mitochondrial dynamics were analyzed as follows. Cells were transiently transfected with a mitochondrial matrix-targeted photoactivable GFP (mito-pA-GFP) that enables detection and quantification of organelle fusion in living cells by confocal microscopy [30]. A decrease in fluorescence applies as a proportion for fission and fusion events, because the decrease reflects the fluorescence diffusion to adjacent mitochondria, supposedly through fusion (for an example, see Fig. 6a). Interestingly, 30 as well as 50–60 min after photoactivation the P301L cells displayed significant higher fluorescence intensity than control cells, meaning that they have a lower fission and fusion rate (Fig. 6b). Setting the intensity directly after activation as 100 % the fluorescence intensity was strongly reduced after 30 and 50–60 min in control cells and wt tau cells (only results after 50–60 min are shown in Fig. 6b). This further strengthens the view that the mitochondrial impairments of P301L cells are coupled to diminished mitochondrial dynamics. Again, fusion and fission rate in wt cells were not altered compared to vct cells.

Fission and fusion activities can be regulated on the transcriptional level [31, 32]. At the moment several components involved in fission and fusion process are discussed. Mfn1 and Mfn2 together with Opa1 are involved in fusion events in mammalian cells compared to Fis1, Drp1 and MPT18, which are responsible for fission events. Because the P301L cells showed impaired distribution and dynamics of mitochondria, we isolated total RNA, performed semiquantitative RT-PCR for the different fission and fusion factors and compared it with wt tau and control cells, which supports our results from live cell imaging. Compared to control cells all fusion factors are lower expressed in P301L cells (Fig. 6c, e), while in wt tau cells the mRNA levels of the fusion factors were not modified (Fig. 6c, e). As expected, fission factors were significantly reduced in P301L cells (Fig. 6d, e). Interestingly fission factors of wt tau cells tend to result in lower mRNA expression and MPT18 is significantly reduced (Fig. 6d, e), which again correlates properly with the altered mitochondrial morphology (see Fig. 5a–c).

Discussion

Although mitochondrial dysfunction plays an important role in neurodegenerative diseases, very little is known about the impact of tau on mitochondrial function. In this study, we distinguished between the effects from overexpression of wt tau and the P301L mutation. Due to the mutation P301L, the tau protein is phosphorylated faster and to a higher extent than wt tau [33]. Therefore, tau loses its ability to bind microtubules and regulate their dynamics [27, 34, 35].

One major observation of this study is that overexpression of wt tau improved mitochondrial function through an increase in complex I activity, resulting in a hyperpolarized membrane potential and higher ATP levels as well as an increased metabolic activity. In contrast, similar to our previous findings in mice bearing the P301L mutation

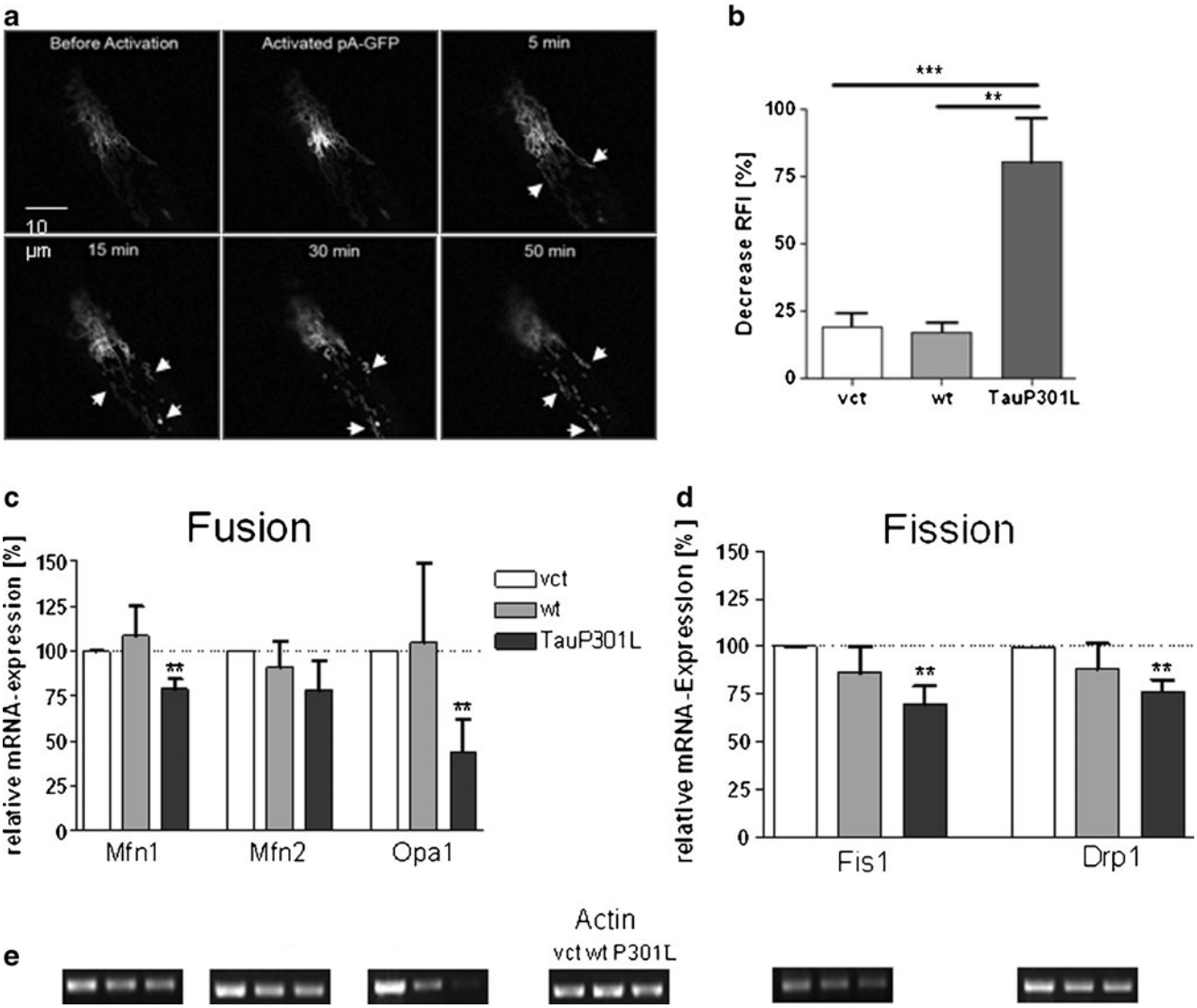

Fig. 6 Fission and fusion is diminished in P301L cells. Diminished fission and fusion rates in P301L cells were detected using photoactivable GFP (mito-pA-GFP) by confocal microscopy and altered mRNA expression of different fusion (Mfn1, Mfn2, Opa1) and fission factors (Fis1, Drp1, MPT18) in tau overexpressing cells. SY5Y cells were transfected 24 h before the measurement with pA-GFP. **a** Confocal microscopy illustrates a course before and after induction of the photoactivable mito-GFP (*pA-GFP*) in wt tau cells. White arrows indicate the distribution of pA-GFP over time course (50 min). **b** Fission and fusion rate at 50–60 min after photoactivation. The background fluorescence before photoactivation of mito-GFP was determined as 0 % and the fluorescence intensity after activation was set as 100 %. Data are mean±SEM, n=5–10; unpaired t-test, $^{**}p<0.01$, $^{***}p<0.001$. **c** Histogram reflecting mRNA expression of fusion factors normalized on actin levels. Data are mean±SEM, n=5–7, unpaired t-test $^{**}p<0.01$. **d** Histogram reflecting quantified fission parameters normalized on actin levels. Data are mean±SEM, n=3–5 (Opa1) n=5–7; unpaired t-test $^{**}p<0.01$. **e** mRNA expression of fission and fusion parameters. Total mRNA was isolated, reverse-transcribed, and subjected to PCR. Data are mean±SEM, n=5–7

mitochondrial dysfunction was detected in cells overexpressing the P301L mutation [8]. We observed decreased ATP level, a slight depolarisation of the MMP as well as decreased metabolic activity induced by a pronounced reduction in complex I activity. These effects on mitochondrial function are not associated with differences in the amount of mitochondria or mtDNA, as measured and compared with control cells. Consistent with our findings, similar numbers of mitochondria were reported in NFT-bearing and non-NFT-bearing cells in AD [36]. In addition, hyperphosphorylated tau seems to be involved in the regulation of oxidative stress [37, 38].

In contrast to opposite complex I activities, the activities of complexes II, III were increased regardless of whether the wt or mutated form was overexpressed while cytochrome *c* oxidase activity was not altered in any cell type, which is consistent with the unaffected complex IV activity in P301L mice [8].

Importantly, these functional changes are paralleled by specific but again opposite ultrastructural changes of mitochondrial morphology in our cell types. The mitochondria from wt tau cells showed the orthodox state with small intracristal spaces while a globular structure of cristae and a dense matrix in mitochondria from cells bearing the P301L mutation was observed. These different structures reflect the physiological status of the cells with high — in wt tau cells — or low ATP levels in P301L cells, respectively. Our results confirm the theory that the surface area of the cristae correlates positively with the ATP level generated from oxidative phosphorylation [39]. A mathematical model from the group of Demongeot et al. [40] proposed that the cristae structure stands for the most effective ATP production, where the distance between adenine translocation and transformation is minimized. Furthermore, the injection of ATP and or ADP into mitochondria revealed the same alterations in the optical density of the matrix and the formation of the cristae [41, 42], as we see in our cell culture.

The changes in mitochondrial ultrastructure could result from an imbalance in mitochondrial fission and fusion. This dynamic process is strongly controlled by the mitochondrial function [14, 43]. Either excessive fission or fusion is considered to negatively affect cell function and viability. Overexpression of wt tau did not affect mitochondrial dynamics with a tendency in downregulation of the fission factors (Fis1, Drp1 and MPT18). Mitochondrial elongation might be the cause for the improved mitochondrial function, as the elongation of mitochondria by downregulation of Fis1 or Drp1 or upregulation of Fzo1A/B (the Mfn1 homolog from rat) in cell culture models conferred resistance to apoptotic stimuli [44, 45]. Thus, the dynamic equilibrium of fission and fusion is adjusted towards fusion, which could be one reason for the extended mitochondrial network. In contrast, the P301L mutation leads to reduced fission and fusion induced by a reduced expression of the fusion factors Mfn1 and OPA1 and all three fission factors. Another important regulator of mitochondrial function and morphology is mitophagy, the degradation of mitochondria by autophagy. Recent data showed that autophagy/mitophagy is upregulated in AD [46, 47]. The authors suggest that mitochondria undergo increased fission in an attempt to segregate damaged mitochondria to degradation by mitophagy. Importantly, stimulation of autophagy reduces neurodegeneration in a mouse model of human tauopathies overexpressing the P301S tau mutation [48].

Beside its effects on mitochondrial function, morphology as well as fission and fusion, tau as an MAP is discussed to spatially regulate the balance of microtubule-dependent axonal transport [3]. In AD, tau accumulates in the somatodendritic compartment. Dixit et al. [3] propose that anterograde transport to the axon is severely compromised finally leading to neurodegeneration. Therefore, we investigated the effects of wt and P301L overexpression on mitochondrial movement which is nearly unchanged in wt tau overexpressing cells. In P301L cells, we observed a significant decrease in mitochondrial movement as we expected according to the hypothesis of Dixit et al. [3]. We propose that overexpression of wt tau leads to a stabilization of the microtubules through binding of dynactin thereby stabilizing its binding to microtubules and indirectly also the transport of vesicles and organelles [3]. Additionally, tau can interact with the plasma membrane or through the dynactin/dynein complex with the actin cytoskeleton and influence the morphology of neurons [49, 50]. Compared to this, the mutation P301L is known to destabilize the microtubule network [27, 33, 35], which leads to a perinuclear localisation of the mitochondria — as seen in our cell model — and to decreased dynamics of microtubules affecting the transport of vesicles and organelles.

Taken together, our findings suggest a pronounced impact of tau on mitochondrial morphology, dynamics and energy metabolism. To our knowledge, we could show for the first time that the overexpression of wt tau has protective effects on mitochondrial morphology and function. On the other hand, the mutation P301L has adverse effects and decreased mitochondrial activity and cause fewer mitochondrial dynamics as well as less fission and fusion. Moreover, the ultrastructure and morphology of the mitochondria reflect their physiological status. However, it remains open if the reduced complex I activity in P301L cells leads to decreased fusion and fission activity and changed mitochondrial morphology as described for complex II inhibition by the Liot et al. [51], or whether the decreased expression of several fusion and fission factors finally results in the reduced complex I activity and the reduced metabolic activity shown by Chen et al. [52]. Mitochondrial and synaptic dysfunction is increasingly considered a major pathogenic pathway in several neurodegenerative and psychiatric disorders triggered very early in the disease process. Our findings clearly link tau pathology mediated toxic effects on mitochondrial function and dynamics, giving a novel sight on the integrity of our brain and neurodegeneration in tauopathies.

Materials and Methods

Cell Culture

Stably transfected human SH-SY5Y neuroblastoma cells with wt and P301L tau were kindly provided by Jürgen Götz, Brain & Mind Research Institute, University of Sydney, Australia [20]. The transfected cells vct, wt tau and P301L tau were cultured in Dulbecco's modified Eagle's medium F12 (DMEM F12; Sigma, http://www.sigmaaldrich.com)

supplemented with 10 % heat-inactivated fetal calf serum and 5 % heat-inactivated horse serum, 50 units/ml penicillin, 50 μg/ml streptomycin and 125 μg/ml G418 at 37 °C in a humidified incubator containing 5 % CO_2. Cells were plated the day before incubation with 100 μM H_2O_2 started for 24 h. Values are expressed as percentages relative to their unstimulated control (=100 %).

Metabolic Activity

This assay allow to measure metabolic activity and is based on the cleavage of the yellow tetrazolium salt, 3-(4,5-dimethylthiazol-2-yl)-2,5-diphenyltetrazoliumbromid (MTT; Sigma) into purple formazan by metabolically active cells, dependent on the pyridine nucleotide cofactors NADH and NADPH. After incubation with different stressors, MTT was added to the 96-well cultures to a final concentration of 1 mg/ml. and incubation was continued for another 2 h. The formazan crystals were solubilised by adding 100 μl of a 20 % SDS in (1:1) *N*,*N*-dimethly-formamide/water solution and incubating overnight at 37 °C [53]. Absorbance was measured at 560 nm with a 620-nm reference wavelength in an ELISA microplate reader.

ATP Levels

SH-SY5Y cells were plated the day before at a density of 2.5×10^4 cells/well in a white 96-well plate and were then incubated for 24 h with different complex inhibitors or 100 μM H_2O_2. ATP levels were determined with a bioluminescence assay (ViaLight HT; Cambrex Bio Science). The enzyme luciferase, which catalyzes the formation of light from ATP and luciferin, was utilized. The emitted light was linearly related to the ATP concentration and measured using a luminometer [54].

Mitochondrial Membrane Potential, ψ_m

SH-SY5Y cells were plated the day before at a density of 1×10^5 cells/well in a 48-well plate and were then incubated for 24 h with 100 μM H_2O_2. The MMP was measured using the fluorescence dye Rhodamine 123 [55] and the dye was added to the cell culture medium in a concentration of 0.4 μM for 15 min. The cells were washed twice with PBS, and the fluorescence was determined with a Victor^2 multiplate reader (PerkinElmer Life Sciences) at 490/535 nm. Loading capacity of the dye within the membrane decreases when the MMP declines after damage.

Enzymatic Determination

Assays of all respiratory chain enzyme activities were carried out spectrophotometrically on a Shimadzu Multi-Spec-1501 diode array spectrophotometer, using standardized and reproducible methods. All activities are expressed in nmol/min/mg and all complex activities were normalized to the citrate synthase activity of the mitochondrial preparation and are given as Complex/CS ratio.

Complex I Activity

Isolated mitochondria (300 μg/assay) were solubilised in *n*-dodecyl-D-maltoside (20 %) (Sigma-Aldrich). To determine NADH–ubiquinone oxidoreductase activity, 100 μM *n*-decylubiquinone (DBQ) and 100 μM NADH were used as substrates, as described previously [56]. Oxidation rates of NADH were recorded with an extinction coefficient $\varepsilon_{340–400\ nm}=6.1\ mM^{-1}\ cm^{-1}$.

Complex II Activity

The assay was performed by following the decrease in absorbance at 600 nm resulting from the reduction of 2,6-dichlorophenolindo-phenol (DCIP) in 1 ml of medium containing 60 mM KH_2PO_4 (pH 7.4), 3 mM KCN, 20 μg/ml rotenone, 20 mM succinate, and 20 μg mitochondrial protein. The reaction was initiated by the addition of 1.3 mM phenazine methasulfate (PMS) and 0.18 mM DCIP as described previously [57]. The extinction coefficient used for DCIP was 21 $mM^{-1}\ cm^{-1}$.

Complex III Activity

The oxidation of 50 μM decylubiquinol obtained by complex III was determined using cytochrome *c* as an electron acceptor as described previously [58]. Briefly, decylubiquinol is prepared by dissolving decylubiquinone (10 mM) in ethanol acidified to pH 2. The quinone is reduced with excess solid sodium borohydride. Decylubiquinol is extracted into diethylether/cyclohexane (2:1, v/v) and evaporated to dryness under nitrogen gas, dissolved in ethanol acidified to pH 2. The assay was carried out in a medium containing 35 mM KH_2PO_4, 5 mM $MgCl_2$, 2 mM KCN (pH 7.2), supplemented with 2.5 mg/ml BSA, 15 μM cytochrome *c*, 0.6 mM *n*-dodecyl β-D-maltoside and 5 μg/ml rotenone. The reaction was started with 10 μg mitochondrial protein and the enzyme activity was measured at 550 nm. The extinction coefficient used for cytochrome *c* was 18.5 $mM^{-1}\ cm^{-1}$.

Complex IV Activity

Cytochrome *c* oxidase activity was determined in intact isolated mitochondria (100 μg/assay) using the Cytochrome *c* Oxidase Assay Kit. The colorimetric assay is

based on the observation that a decrease in absorbance at 550 nm of ferrocytochrome *c* is caused by its oxidation to ferricytochrome *c* by cytochrome *c* oxidase. The Cytochrome *c* Oxidase Assay was performed as described previously [59].

Citrate Synthase Activity

The reduction of 5,5-dithiobis(2-nitrobenzoicacid) by citrate synthase at 412 nm (extinction coefficient of 13.6 mM^{-1} cm^{-1}) was followed in a coupled reaction with coenzyme A and oxaloacetate. A reaction mixture of 0.2 M Tris–HCl, pH 8.0, 0.1 mM acetyl-coenzyme A, 0.1 mM 5,5-dithiobis(2-nitrobenzoicacid), *n*-dodecyl-β-D-maltoside (20 %) and 10 μg mitochondrial protein was incubated at 30 °C for 5 min. The reaction was initiated by the addition of 0.5 mM oxaloacetate, and the absorbance change was monitored for 5 min.

Confocal Microscopy and Image Analysis

Mitochondria were visualized with MitoTracker Deep Red for live cell experiments and with MitoTracker CMXRos for PFA-fixed probes (Molecular Probes), at a final concentration of 25 nM for 30 min and nuclei stained with Höchst33258. Micrographs were taken with a Leica SP 5 confocal laser scanning microscope (Leica, Wetzlar, Germany) fitted with the appropriate filters and a plan-apochromate 63×, 1.4 NA. Live cell experiments were performed at 37 °C and 5 % CO_2 in a humidified chamber. For mitochondrial movement studies, a picture was made every 1.5 s over 2 min and the increase in gray scales was calculated compared to the first picture. To study fission and fusion of mitochondria a method from the group of Youle was modified [30]. In brief, cells were transfected with mitochondrial pA-GFP (Fugene) and 405- or 413-nm light was used for photoactivation of pA-GFP [60]. ROIs were selected, irradiated with 405- or 413-nm light and images were taken over 50 to 60 min. Postacquisition processing was performed with ImageJ software, Microsoft Excel, and Adobe Photoshop.

Electron Microscopy

Transfected cells were trypsinized, chemically fixed by addition of a freshly made solution of PBS containing 3.7 % (w/v) formaldehyde and 0.5 % (v/v) glutaraldehyde, incubated for 1 h at room temperature, and washed twice with PBS. After aldehyde fixation samples were postfixed with 1 % osmic acid in 0.1 M sodium cacodylate buffer (pH 7.2), washed in water, incubated over night in 1 % uranyl acetate, washed first in 0.05 M acetate buffer, then in water and thereafter dehydrated by a series of increasing concentrations of ethanol. Next samples were infiltrated with Agar LV Premix Kit (Agar Scientific Ltd. ordered from Plano, Wetzlar, Germany) resin embedding medium and polymerized by heat (65 °C, 16 h). Thin sections were cut with an ultramicrotome (Ultracut, Leica Instruments GmbH, Nussloch), double contrasted with uranyl acetate and lead citrate and afterwards viewed the electron microscope EM208S (FEI company) equipped with an 1 k×1 k slow scan CCD camera (TVIPS, Munich, Germany).

RNA Isolation and Semiquantitative RT-PCR

Total RNA was isolated from 3 to 5×10^6 non-treated SH-SY5Y cells with Trizol (Invitrogen), according to the manufacturers' instructions. Two micrograms of total RNA were used for first strand synthesis with oligo(dT) and random hexamer primers. Expression of fission and fusion factor transcripts was analysed in a semiquantitative polymerase chain reaction (PCR), with β-actin for normalization. Primer: β-actin: 5′-CCACC CATGGCAAATTCCAT GGCA-3′ (sense) and 5′-TCTA GACGGCAGGTCAGGTCCACC-3′ (antisense); Mfn1: 5′-CTCCAGCAACGCCAGATAATGC-3′ (sense) and 5′-ACTTGTTGGCACAGGCGAGC-3′ (antisense); Mfn2: 5′-GGATGCTGATGTGTTTGTGCTGG-3′ (sense) and 5′-AGTCCATGATGAGTCGAACCGC-3′ (antisense); Opa1: 5′-GGCTCTGCAGGCTCGTCTCA AGG-3′ (sense) and 5′-TTCCGCCAGTTGAACGCGTTTACC-3′ (antisense), Fis1: 5′-CGAGCTGGTGTCTGTGGAGGACC-3′ (sense) and 5′-TGTCAATGAGCCGCTCCAGTTCC-3′ (antisense); Drp1: 5′-AACTTGATCTCATGGATGCGGG-3′ (sense) and 5′-ATGAACCAGTTCCACACAGCGG-3′ (antisense).

mtDNA Copies for Mitochondrial Mass

For quantitative real-time PCR, total DNA was isolated from 1×10^6 cells with the DNA Flexi Kit (Qiagen). The primers for RT Q-PCR analysis of mtDNA are mtF3212 (5′-CACCCAA GAACAGGGTTTGT-3′) and mtR3319 (5′-TGGCCATGGG TATGTTGTTAA-3′) [61] and those for the nuclear gene (nDNA) for the human polymerase γ accessory subunit (ASPOLG), ASPG3F (5′-GAGCTGTTGACGGAAAG GAG-3′) and ASPG4R (5′-CAGAAGAGAATCCCGGC TAAG-3′) [62]. The 20 μl PCR reaction contains 10 μl Power SYBR Green Master Mix (Applied Biosystems), 1 μM of each primer, and 10 ng of total genomic DNA extract. PCR conditions are an initial denaturation of 10 min at 95 °C, followed by 40 cycles of 15 s of denaturation at 95 °C and 60 s of annealing/extension at 60 °C. All experiments were done in 96-well optical plates on a StepOnePlus© Real-Time PCR System (Applied Biosystems). Fluorescence was measured at the end of each extension step. The results from the quantitative PCR were expressed as the ratio of the mean mitochondrial DNA value of duplicate measurements to the mean nuclear DNA value of duplicate measurements for a given extract (mtDNA/nDNA).

Western Blot

Equal amounts (15 μg) of protein were loaded on a 10 % NuPAGE gel (Invitrogen, Germany) and proteins were separated as previously described [20]. Briefly, probes were transferred onto a nitrocellulose membrane (Amersham Biosciences, Germany). Equal protein loading was confirmed by Ponceau Red staining (Sigma, Germany). Membranes were saturated with 3 % nonfat dry milk for 1 h, washed three times with TBST and incubated with the primary antibody (mouse anti TAU clone HT7; Innogenetics, 1:1,000), overnight at 4 °C. After washing with TBST, membranes were treated with the horseradish-coupled secondary antibody (anti-mouse HRP, Calbiochem, Germany; 1:1,000).

Immunostaining

Cells were plated at a density of 4×10^5 cells on collagen treated coverslips. After 2 days growing, coverslips were fixed in PBS with 4 % paraformaldehyde for 30 min, then permeabilized with 0.1 % Triton for 15 min and blocked with PBS 10 % goat serum for 1 h at 37 °C. The coverslips were incubated for 1 h at 37 °C with the primary antibody (Anti-Human PHF TAU Clone HT7, Innogenetics; 1:100). After washing with PBS, they were incubated for 30 min at 37 °C with the secondary antibody (anti-mouse IgG (Fab Specific) FITC, Sigma, Switzerland, 1:500). Staining was assessed using a Zeiss Axiolab microscope.

Acknowledgements The authors thank M. Vöth for support with the mitochondrial movement data analysis, F. Haas for experimental support with the real-time PCR and F. Meier with regard to Western blotting. This work was supported in part by grants from the Swiss National Research Foundation (SNF # 31000_122572) and Synapsis Foundation to AE, by the DFG grant REI1575-1/1 (AR), he Cluster of Excellence Frankfurt Macromolecular Complexes at the University of Frankfurt DFG project EXC 115 (AR), and the BMBF, Germany, GerontoMitoSys project (AR).

References

1. Spires-Jones TL, Stoothoff WH, de Calignon A, Jones PB, Hyman BT (2009) Tau pathophysiology in neurodegeneration: a tangled issue. Trends Neurosci 3:150–159
2. Goedert M, Wischik CM, Crowther RA, Walker JE, Klug A (1988) Cloning and sequencing of the cDNA encoding a core protein of the paired helical filament of Alzheimer disease: identification as the microtubule-associated protein tau. Proc Natl Acad Sci U S A 11:4051–4055
3. Dixit R, Ross JL, Goldman YE, Holzbaur EL (2008) Differential regulation of dynein and kinesin motor proteins by tau. Science 5866:1086–1089
4. Hutton M, Lendon CL, Rizzu P, Baker M, Froelich S, Houlden H, Pickering-Brown S, Chakraverty S, Isaacs A, Grover A et al (1998) Association of missense and 5′-splice-site mutations in tau with the inherited dementia FTDP-17. Nature 6686:702–705
5. Poorkaj P, Bird TD, Wijsman E, Nemens E, Garruto RM, Anderson L, Andreadis A, Wiederholt WC, Raskind M, Schellenberg GD (1998) Tau is a candidate gene for chromosome 17 frontotemporal dementia. Ann Neurol 6:815–825
6. Spillantini MG, Murrell JR, Goedert M, Farlow MR, Klug A, Ghetti B (1998) Mutation in the tau gene in familial multiple system tauopathy with presenile dementia. Proc Natl Acad Sci U S A 13:7737–7741
7. von Bergen M, Barghorn S, Li L, Marx A, Biernat J, Mandelkow EM, Mandelkow E (2001) Mutations of tau protein in frontotemporal dementia promote aggregation of paired helical filaments by enhancing local beta-structure. J Biol Chem 51:48165–48174
8. David DC, Hauptmann S, Scherping I, Schuessel K, Keil U, Rizzu P, Ravid R, Drose S, Brandt U, Muller WE et al (2005) Proteomic and functional analyses reveal a mitochondrial dysfunction in P301L Tau transgenic mice. J Biol Chem 25:23802–23814
9. Kuhla B, Loske C, Garcia DA, Schinzel R, Huber J, Munch G (2004) Differential effects of "Advanced glycation endproducts" and beta-amyloid peptide on glucose utilization and ATP levels in the neuronal cell line SH-SY5Y. J Neural Transm 3:427–439
10. Srikanth V, Maczurek A, Phan T, Steele M, Westcott B, Juskiw D, Munch G (2011) Advanced glycation endproducts and their receptor RAGE in Alzheimer's disease. Neurobiol Aging 5:763–777
11. Busch KB, Bereiter-Hahn J, Wittig I, Schagger H, Jendrach M (2006) Mitochondrial dynamics generate equal distribution but patchwork localization of respiratory complex I. Mol Membr Biol 6:509–520
12. Ishihara N, Jofuku A, Eura Y, Mihara K (2003) Regulation of mitochondrial morphology by membrane potential, and DRP1-dependent division and FZO1-dependent fusion reaction in mammalian cells. Biochem Biophys Res Commun 4:891–898
13. Ono T, Isobe K, Nakada K, Hayashi JI (2001) Human cells are protected from mitochondrial dysfunction by complementation of DNA products in fused mitochondria. Nat Genet 3:272–275
14. Suen DF, Norris KL, Youle RJ (2008) Mitochondrial dynamics and apoptosis. Genes Dev 12:1577–1590
15. Detmer SA, Chan DC (2007) Functions and dysfunctions of mitochondrial dynamics. Nat Rev Mol Cell Biol 11:870–879
16. Westermann B (2008) Molecular machinery of mitochondrial fusion and fission. J Biol Chem 20:13501–13505
17. Knott AB, Perkins G, Schwarzenbacher R, Bossy-Wetzel E (2008) Mitochondrial fragmentation in neurodegeneration. Nat Rev Neurosci 7:505–518
18. Wang X, Su B, Fujioka H, Zhu X (2008) Dynamin-like protein 1 reduction underlies mitochondrial morphology and distribution abnormalities in fibroblasts from sporadic Alzheimer's disease patients. Am J Pathol 2:470–482
19. Wang X, Su B, Siedlak SL, Moreira PI, Fujioka H, Wang Y, Casadesus G, Zhu X (2008) Amyloid-beta overproduction causes abnormal mitochondrial dynamics via differential modulation of mitochondrial fission/fusion proteins. Proc Natl Acad Sci USA 49:19318–19323
20. Ferrari A, Hoerndli F, Baechi T, Nitsch RM, Gotz J (2003) beta-Amyloid induces paired helical filament-like tau filaments in tissue culture. J Biol Chem 41:40162–40168
21. Schaeffer V, Patte-Mensah C, Eckert A, Mensah-Nyagan AG (2006) Modulation of neurosteroid production in human neuroblastoma cells by Alzheimer's disease key proteins. J Neurobiol 8:868–881
22. Letellier T, Durrieu G, Malgat M, Rossignol R, Antoch J, Deshouillers JM, Coquet M, Lacombe D, Netter JC, Pedespan JM et al (2000) Statistical analysis of mitochondrial pathologies in childhood: identification of deficiencies using principal component analysis. Lab Invest 7:1019–1030
23. Leuner K, Hauptmann S, Abdel-Kader R, Scherping I, Keil U, Strosznajder JB, Eckert A, Muller WE (2007) Mitochondrial dysfunction: the first domino in brain aging and Alzheimer's disease? Antioxid Redox Signal 10:1659–1675

24. Bai RK, Perng CL, Hsu CH, Wong LJ (2004) Quantitative PCR analysis of mitochondrial DNA content in patients with mitochondrial disease. Ann N Y Acad Sci 304–309
25. Schneider WC, Hogeboom GH (1951) Cytochemical studies of mammalian tissues; the isolation of cell components by differential centrifugation: a review. Cancer Res 1:1–22
26. Baloyannis SJ (2006) Mitochondrial alterations in Alzheimer's disease. J Alzheimers Dis 2:119–126
27. Bunker JM, Kamath K, Wilson L, Jordan MA, Feinstein SC (2006) FTDP-17 mutations compromise the ability of tau to regulate microtubule dynamics in cells. J Biol Chem 17:11856–11863
28. Ebneth A, Godemann R, Stamer K, Illenberger S, Trinczek B, Mandelkow E (1998) Overexpression of tau protein inhibits kinesin-dependent trafficking of vesicles, mitochondria, and endoplasmic reticulum: implications for Alzheimer's disease. J Cell Biol 3:777–794
29. Roy S, Zhang B, Lee VM, Trojanowski JQ (2005) Axonal transport defects: a common theme in neurodegenerative diseases. Acta Neuropathol 1:5–13
30. Karbowski M, Arnoult D, Chen H, Chan DC, Smith CL, Youle RJ (2004) Quantitation of mitochondrial dynamics by photolabeling of individual organelles shows that mitochondrial fusion is blocked during the Bax activation phase of apoptosis. J Cell Biol 4:493–499
31. Honda S, Hirose S (2003) Stage-specific enhanced expression of mitochondrial fusion and fission factors during spermatogenesis in rat testis. Biochem Biophys Res Commun 2:424–432
32. Jendrach M, Mai S, Pohl S, Voth M, Bereiter-Hahn J (2008) Short- and long-term alterations of mitochondrial morphology, dynamics and mtDNA after transient oxidative stress. Mitochondrion 4:293–304
33. Alonso AC, Mederlyova A, Novak M, Grundke-Iqbal I, Iqbal K (2004) Promotion of hyperphosphorylation by frontotemporal dementia tau mutations. J Biol Chem 279:34873–34881
34. Hasegawa M, Smith MJ, Goedert M (1998) Tau proteins with FTDP-17 mutations have a reduced ability to promote microtubule assembly. FEBS Lett 3:207–210
35. Hong M, Zhukareva V, Vogelsberg-Ragaglia V, Wszolek Z, Reed L, Miller BI, Geschwind DH, Bird TD, McKeel D, Goate A et al (1998) Mutation-specific functional impairments in distinct tau isoforms of hereditary FTDP-17. Science 5395:1914–1917
36. Sumpter PQ, Mann DM, Davies CA, Yates PO, Snowden JS, Neary D (1986) An ultrastructural analysis of the effects of accumulation of neurofibrillary tangle in pyramidal neurons of the cerebral cortex in Alzheimer's disease. Neuropathol Appl Neurobiol 3:305–319
37. Bonda DJ, Castellani RJ, Zhu X, Nunomura A, Lee HG, Perry G, Smith MA (2011) A novel perspective on tau in Alzheimer's disease. Curr Alzheimer Res 6:639–642
38. Su B, Wang X, Lee HG, Tabaton M, Perry G, Smith MA, Zhu X (2010) Chronic oxidative stress causes increased tau phosphorylation in M17 neuroblastoma cells. Neurosci Lett 3:267–271
39. Palade GE (1953) An electron microscope study of the mitochondrial structure. J Histochem Cytochem 4:188–211
40. Demongeot J, Glade N, Hansen O, Moreira A (2007) An open issue: the inner mitochondrial membrane (IMM) as a free boundary problem. Biochimie 9:1049–1057
41. Hackenbrock CR (1968) Chemical and physical fixation of isolated mitochondria in low-energy and high-energy states. Proc Natl Acad Sci USA 2:598–605
42. Bereiter-Hahn J, Voeth M. (1983) Metabolic control of shape and structure of mitochondria *in situ*. Biol Cell 1042:304–309
43. Knott AB, Bossy-Wetzel E (2008) Impairing the mitochondrial fission and fusion balance: a new mechanism of neurodegeneration. Ann N Y Acad Sci 1147:283–292
44. Lee YJ, Jeong SY, Karbowski M, Smith CL, Youle RJ (2004) Roles of the mammalian mitochondrial fission and fusion mediators Fis1, Drp1, and Opa1 in apoptosis. Mol Biol Cell 11:5001–5011
45. Sugioka R, Shimizu S, Tsujimoto Y (2004) Fzo1, a protein involved in mitochondrial fusion, inhibits apoptosis. J Biol Chem 50:52726–52734
46. Moreira PI, Siedlak SL, Wang X, Santos MS, Oliveira CR, Tabaton M, Nunomura A, Szweda LI, Aliev G, Smith MA et al (2007) Increased autophagic degradation of mitochondria in Alzheimer disease. Autophagy 6:614–615
47. Moreira PI, Siedlak SL, Wang X, Santos MS, Oliveira CR, Tabaton M, Nunomura A, Szweda LI, Aliev G, Smith MA et al (2007) Autophagocytosis of mitochondria is prominent in Alzheimer disease. J Neuropathol Exp Neurol 6:525–532
48. Schaeffer V, Lavenir I, Ozcelik S, Tolnay M, Winkler DT, Goedert M (2012) Stimulation of autophagy reduces neurodegeneration in a mouse model of human tauopathy. Brain Pt 7:2169–2177
49. Brandt R, Leger J, Lee G (1995) Interaction of tau with the neural plasma membrane mediated by tau's amino-terminal projection domain. J Cell Biol 5:1327–1340
50. Magnani E, Fan J, Gasparini L, Golding M, Williams M, Schiavo G, Goedert M, Amos LA, Spillantini MG (2007) Interaction of tau protein with the dynactin complex. EMBO J 21:4546–4554
51. Liot G, Bossy B, Lubitz S, Kushnareva Y, Sejbuk N, Bossy-Wetzel E (2009) Complex II inhibition by 3-NP causes mitochondrial fragmentation and neuronal cell death via an. Cell Death Differ 16:899–909
52. Chen H, McCaffery JM, Chan DC (2007) Mitochondrial fusion protects against neurodegeneration in the cerebellum. Cell 3:548–562
53. Hansen MB, Nielsen SE, Berg K (1989) Re-examination and further development of a precise and rapid dye method for measuring cell growth/cell kill. J Immunol Methods 2:203–210
54. Crouch SP, Kozlowski R, Slater KJ, Fletcher J (1993) The use of ATP bioluminescence as a measure of cell proliferation and cytotoxicity. J Immunol Methods 1:81–88
55. Baracca A, Sgarbi G, Solaini G, Lenaz G (2003) Rhodamine 123 as a probe of mitochondrial membrane potential: evaluation of proton flux through F(0) during ATP synthesis. Biochim Biophys Acta 1–3:137–146
56. Djafarzadeh R, Kerscher S, Zwicker K, Radermacher M, Lindahl M, Schagger H, Brandt U (2000) Biophysical and structural characterization of proton-translocating NADH–dehydrogenase (complex I) from the strictly aerobic yeast *Yarrowia lipolytica*. Biochim Biophys Acta 1:230–238
57. Aleardi AM, Benard G, Augereau O, Malgat M, Talbot JC, Mazat JP, Letellier T, Dachary-Prigent J, Solaini GC, Rossignol R (2005) Gradual alteration of mitochondrial structure and function by beta-amyloids: importance of membrane viscosity changes, energy deprivation, reactive oxygen species production, and cytochrome *c* release. J Bioenerg Biomembr 4:207–225
58. Krahenbuhl S, Chang M, Brass EP, Hoppel CL (1991) Decreased activities of ubiquinol:ferricytochrome *c* oxidoreductase (complex III) and ferrocytochrome *c*:oxygen oxidoreductase (complex IV) in liver mitochondria from rats with hydroxycobalamin[c-lactam]-induced methylmalonic aciduria. J Biol Chem 31:20998–21003
59. Rasmussen UF, Rasmussen HN (2000) Human quadriceps muscle mitochondria: a functional characterization. Mol Cell Biochem 1–2:37–44
60. Patterson GH, Lippincott-Schwartz J (2002) A photoactivatable GFP for selective photolabeling of proteins and cells. Science 5588:1873–1877
61. Bai RK, Perng CL, Hsu CH, Wong LJ (2004) Quantitative PCR analysis of mitochondrial DNA content in patients with mitochondrial disease. Ann N Y Acad Sci 1042:304–309
62. Cote HC, Brumme ZL, Craib KJ, Alexander CS, Wynhoven B, Ting L, Wong H, Harris M, Harrigan PR, O'Shaughnessy MV et al (2002) Changes in mitochondrial DNA as a marker of nucleoside toxicity in HIV-infected patients. N Engl J Med 11:811–820